

Temperature and Humidity Stable Alkali/Alkaline-Earth Metal Carbonates as Electron Heterocontacts for Silicon Photovoltaics

Yimao Wan,* James Bullock, Mark Hettick, Zhaoran Xu, Chris Samundsett, Di Yan, Jun Peng, Jichun Ye, Ali Javey, and Andres Cuevas

Nanometer scale interfacial layers between the metal cathode and the n-type semiconductor play a critical role in enhancing the transport of charge carriers in and out of optoelectronic devices. Here, a range of nanoscale alkali and alkaline earth metal carbonates (i.e., potassium, rubidium, caesium, calcium, strontium, and barium) are shown to function effectively as electron heterocontacts to lightly doped n-type crystalline silicon (c-Si), which is particularly challenging to contact with common metals. These carbonate interlayers are shown to enhance the performance of n-type c-Si proof-of-concept solar cells up to a power conversion efficiency of $\approx 19\%$. Furthermore, these devices are thermally stable up to $350\text{ }^{\circ}\text{C}$ and both the caesium and barium carbonates pass a standard 1000 h damp heat test, with $>95\%$ of their initial performance maintained. The temperature and humidity stable electron heterocontacts based on alkali and alkaline earth metal carbonates show a high potential for industrial feasibility and longevity for deployment in the field.

A key metric of a metal to silicon contact is the barrier height, predicted by the Schottky-Mott rule to be the difference between the metal work function and silicon's electron affinity.^[1,2] Usually, the observed barrier height differs significantly from the calculated one, due to the Fermi-level pinning phenomenon,

a consequence of a high density of states within the energy bandgap at the metal/silicon interface. Besides the conventional approach of heavily doping the silicon surface in order to make the Schottky barrier thin enough for carrier tunneling, an alternative approach is to employ a thin interfacial layer between metal and silicon to reduce the defect density at the interface, thus releasing the Fermi level. This means, on the one hand, that the work function of the contacting materials needs to be carefully selected for either n-type or p-type silicon; on the other hand, the defect-passivating interlayer can hinder the transport of carriers. For a low-resistance Ohmic contact to n-type silicon (n-Si), it is desirable that the interfacial layer also has the function of reducing the work function of the outer metal in order to facilitate electron ejection (in the

case of solar cells) or injection (for other devices). Recently, several dopant-free interfacial materials have been shown to provide a low resistivity Ohmic contact to n-Si, including lithium fluoride,^[3–5] magnesium fluoride,^[6] magnesium oxide,^[7] titanium oxide,^[8,9] tantalum oxide,^[10] and their combinations.^[11]

Another class of candidate materials is the alkali and alkaline-earth metal carbonates which until now have mostly been explored in organic electronics due to their ability to facilitate electron injection. The application of these carbonates to silicon solar cells is only incipient and it has been limited to caesium carbonate.^[12,13] In this work, we present a comprehensive experimental study of a range of carbonates ($\text{K}_2\text{C}_x\text{O}_y$, $\text{Rb}_2\text{C}_x\text{O}_y$, $\text{Cs}_2\text{C}_x\text{O}_y$, CaC_xO_y , SrC_xO_y , and BaC_xO_y) as electron contacts for silicon solar cells. We first investigate the electronic band structure and conduction properties of the thermally evaporated carbonates. After optimizing these electron contacts in terms of contact resistivity, they are applied to the full rear surface of n-type silicon solar cells, achieving a fill factor (FF) of $\approx 80\%$ and a power conversion efficiency (PCE) up to $\approx 19.4\%$. Thermal and environmental stability tests are then performed, showing that these devices are stable up to $350\text{ }^{\circ}\text{C}$ and that both the caesium and barium carbonates pass an accelerated environmental test at $85\text{ }^{\circ}\text{C}$ and 85% humidity for 1000 h.

The electronic band structure was characterized via X-ray photoelectron spectroscopy (XPS), including core level and

Dr. Y. Wan, C. Samundsett, Dr. D. Yan, J. Peng, Prof. A. Cuevas
Research School of Engineering
The Australian National University (ANU)
Canberra, ACT 0200, Australia
E-mail: yimao.wan@anu.edu.au

Dr. Y. Wan, Dr. J. Bullock, M. Hettick, Z. Xu, Prof. A. Javey
Department of Electrical Engineering and Computer Sciences
University of California
Berkeley, CA 94720, USA

Dr. Y. Wan, Dr. J. Bullock, M. Hettick, Z. Xu, Prof. A. Javey
Materials Sciences Division
Lawrence Berkeley National Laboratory
Berkeley, CA 94720, USA

Prof. J. Ye
Ningbo Institute of Material Technology and Engineering
Chinese Academy of Sciences
Ningbo 315201, China

 The ORCID identification number(s) for the author(s) of this article can be found under <https://doi.org/10.1002/aenm.201800743>.

DOI: 10.1002/aenm.201800743

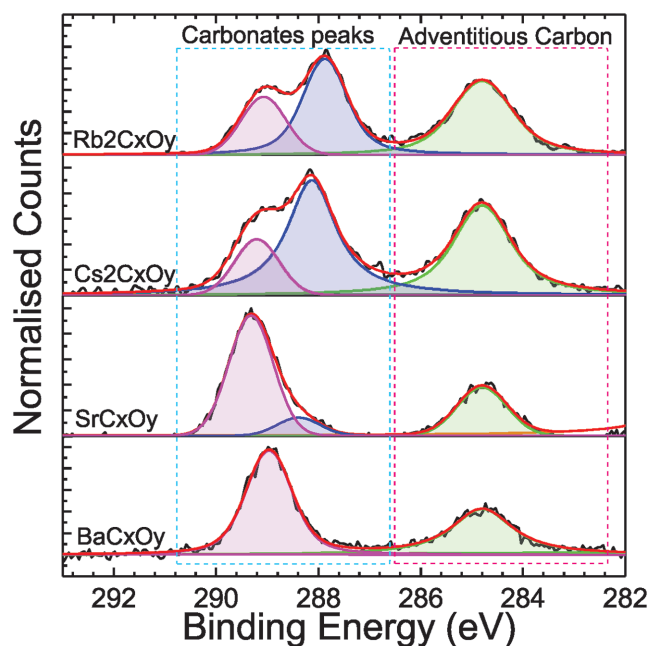


Figure 1. The core level spectrum of C1s of thermally evaporated carbonate films measured by X-ray photoelectron spectroscopy (XPS) measurements. The extracted stoichiometry is summarized in Table 1. The spectra are provided for four of the carbonates. Potassium and calcium carbonates are not included because of their poor stability in air and even in a nitrogen glove box.

valence band analysis. **Figure 1a** shows the core levels of C 1s spectra for four of the carbonates, except for the case of potassium and calcium because of their extremely poor stability in air and even in a nitrogen glove box, owing to the loose packing of relatively large carbonate anions and small metal ions.^[14] The C 1s spectrum is composed of three parts: the main carbonate at ≈ 289.5 eV, the hydrocarbonate at ≈ 288 eV, and the adventitious carbon at ≈ 285 eV.^[15] All four materials exhibit significant adventitious carbon, likely due to organic contaminants during evaporation, transportation, and/or measurement. The hydrocarbonate signal is anticipated to originate from the interaction with environmental moisture. The signal is more pronounced for alkali carbonates than alkaline earth carbonates. This is within expectations, since alkali carbonates are much more hygroscopic.^[14] Particularly for Ba carbonate, the signal for hydrocarbonate is negligible, indicating that the material is more stable against moisture or air ambient, which is supported by the environmental tests at the device level presented below. It is worth noting that the pronounced carbon component observed in this work contradicts previous reports for Cs_2CO_3 , which mention its decomposition into caesium oxide, with negligible release of carbon.^[16] The discrepancy might originate from a different degree of decomposition of Cs_2CO_3 during thermal evaporation. The stoichiometry of the four films measured by XPS is summarized in **Table 1**. It shows that the composition of the alkali carbonates is richer in C and O than the alkaline earth metal ones, presumably due to their higher hygroscopicity. It is also noticeable that the stoichiometry of the alkaline earth metal carbonates is slightly metal rich.

Table 1. Summary of stoichiometry and work function of thermally evaporated carbonates.

Material	Stoichiometry		Work function [eV]
	x	y	
$\text{Rb}_2\text{C}_x\text{O}_y$	1.23	4.48	2.66
$\text{Cs}_2\text{C}_x\text{O}_y$	0.87	3.09	2.36
SrC_xO_y	0.55	2.92	2.81
BaC_xO_y	0.59	2.51	2.23

The work function of the four carbonates is determined by the XPS secondary electron cutoff measurement. The results shown in **Figure 2a** and summarized in Table 1 indicate that all four carbonates exhibit an extremely low work function, ranging from 2.23 to 2.81 eV, in good agreement with the value for Cs_2CO_3 (≈ 2.2 eV) reported by Huang et al.^[16] These results demonstrate their ability to strongly reduce the work function of the carbonate/Al contact, which for pure Al is ≈ 4.1 eV.^[2] The reduced work function is anticipated to promote downward band-bending inside the silicon wafer, drawing electrons to the surface and consequently improving electron transport, as illustrated schematically in **Figure 2b**.

The electrical contact behavior of the carbonate/Al electrodes onto n-Si is evaluated by measuring the contact resistivity ρ_c using the method devised by Cox and Strack,^[17] as shown schematically in the inset of **Figure 2c**. A series of representative current–voltage (I – V) measurements of samples without and with 1 nm of six different carbonate interlayers between Al and n-Si is shown in **Figure 2c**. As we can see in this figure, the sample with Al directly on n-Si (i.e., without a carbonate interlayer) exhibits a high contact resistivity ρ_c of $\approx 5 \Omega \text{ cm}^2$ and a nonlinear behavior. In contrast, the insertion of a nanoscale carbonate (≈ 1 nm) film enhances the contact substantially. The extracted ρ_c for the six carbonates is plotted as a function of film thickness in **Figure 2d**. It can be seen that, for all the six carbonates explored in this work, the insertion of a 0.5 nm carbonate interlayer induces a dramatic decrease of ρ_c by more than one order of magnitude. The ρ_c reaches a minimum for a film thickness of ≈ 1 nm, and then it increases rapidly for film thickness above 5 nm. This dependence of ρ_c on film thickness is similar to that observed for fluorides and oxides.^[3–7] The likely reasons for the low resistance for electron transport provided by the carbonate/Al contacts could be a combination of the low work function and a reduction of the Fermi level pinning effect. However, the solar cell device results presented below indicate that the level of passivation is relatively modest and, therefore, the low work function is most likely the main contribution for the low contact resistance.

The six different carbonate (≈ 1 nm)/Al (≈ 200 nm) electron contacts were integrated in the complete n-type silicon solar cells as full area rear contacts, as schematically depicted in **Figure 3a**. The current–voltage (J – V) photovoltaic characteristic curves under one sun standard illumination are plotted in **Figure 3b** for cells with and without carbonate interlayers (i.e., the control cell with Al directly on n-Si). The detailed electrical parameters of all the cells are given in **Figure 3c**. As expected from the contact resistance measurements, the insertion of a 1 nm thick interfacial layer enhances substantially all cell

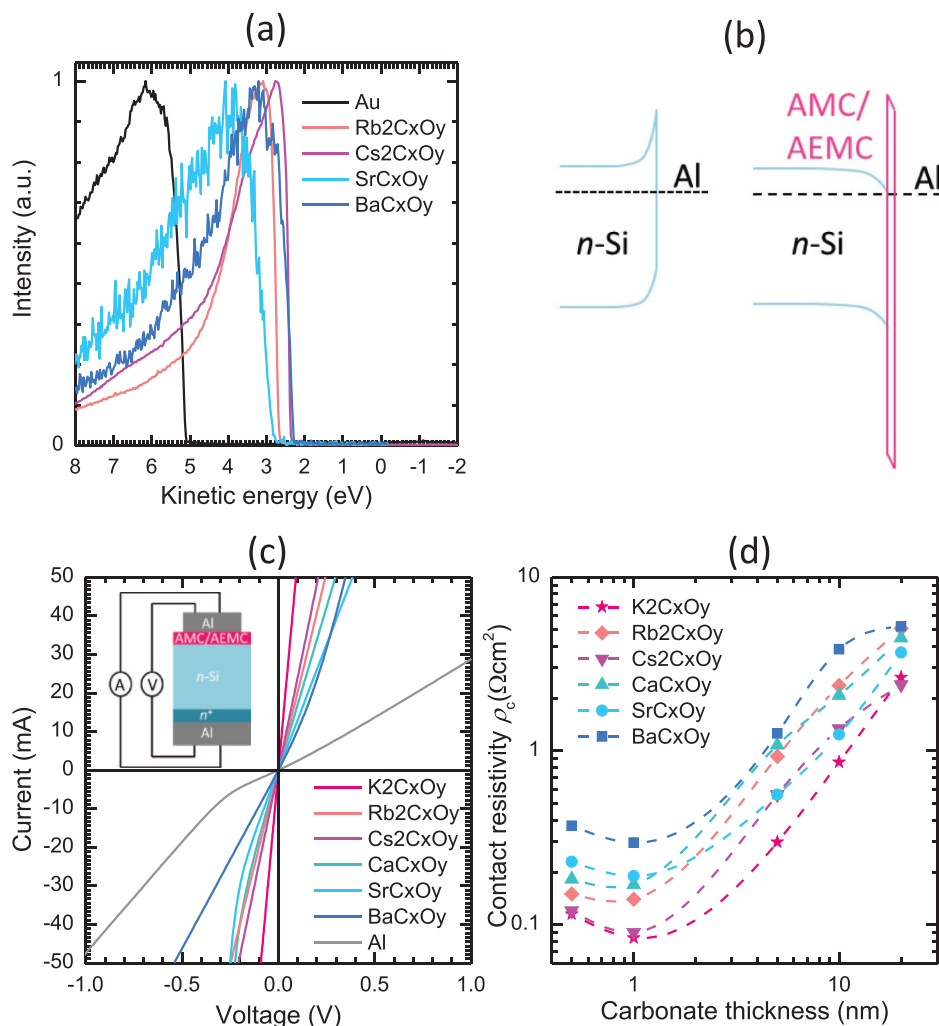


Figure 2. a) shows the secondary electron cutoff spectrum measured on metal carbonates with a gold (Au) reference. b) Provides a schematic of the energy band diagram of a contact with and without carbonate interfacial layers. c) Presents a series of I - V measurements of samples with 1 nm carbonate interlayer between Al and n-type c-Si. A schematic of the contact resistivity test structure is included in the inset. d) Shows the contact resistivity ρ_c as a function of carbonate thickness.

parameters for all six carbonates. The highest power conversion efficiency of 19.4% in this set of experiments is obtained for potassium carbonate, with open-circuit voltage (V_{OC}), short-circuit current (J_{SC}) and FF of 624.3 mV, 38.89 mA cm^{-2} , and 79.94%, respectively. Compared to the control cell (i.e., without a carbonate interlayer), an absolute 30–60 mV increase of V_{OC} is observed for cells with the six carbonates. Although this may be taken as proof of some level of passivation of the silicon surface by the carbonates, it is important to keep in mind that the contact between Al and n-Si in the control cell is not perfectly Ohmic and can originate a small loss of voltage in the device. The fact that the short-circuit current is also higher for the devices with a carbonate/Al contact tends to support the hypothesis of a mild surface passivating effect. Nevertheless, V_{OC} is more sensitive to surface passivation, and the values measured for these cells are not consistent with high quality passivation. Further work should explore the addition of extra interlayers to improve the passivation quality. Another significant gain in cell performance comes from an increase of FF by

an absolute 5.5%, which is directly attributable to the reduction of the contact resistivity presented in Figure 2. Globally, the improvement in V_{OC} , J_{SC} , and FF demonstrates very promising electron selective properties for these alkali and alkaline earth metal carbonates.

For any new contact-formation technology, even if successful in the lab, the thermal stability and environmental reliability of the solar cell devices must also be demonstrated. To investigate this, one set of solar cells with ≈ 1 nm carbonate interlayers was annealed in forming gas for 10 min at different temperatures in the range 250–500 °C, whereas another set was submitted to a standard 1000 h damp heat test at 85 °C and 85% relative humidity. The relative change of the electrical parameters of the solar cells with respect to the control devices before treatment is plotted in Figure 4a,b for the two tests, respectively. As can be seen in Figure 4a, the cell parameters are essentially stable up to 350 °C for all the carbonates, and then start deteriorating when the annealing temperature is increased further. It is worth mentioning that we do not observe a significant difference

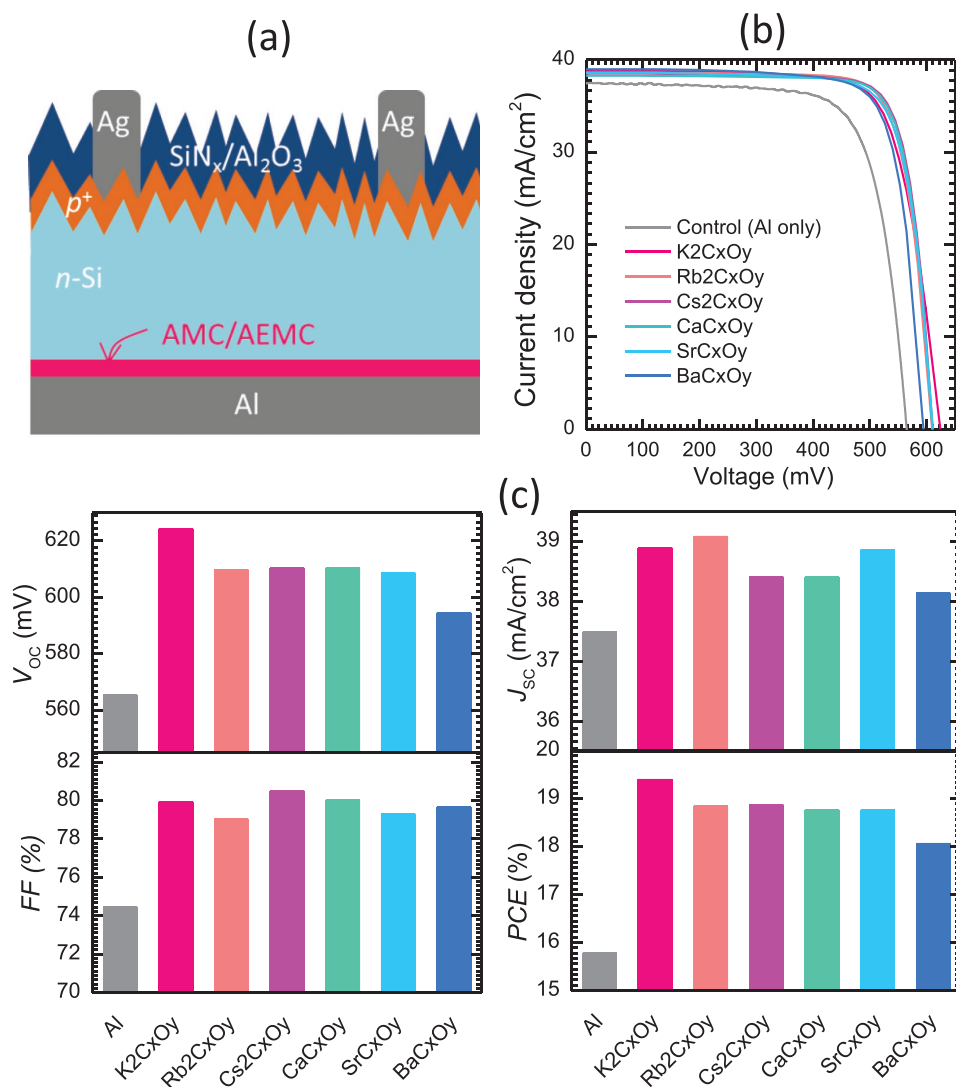


Figure 3. a) Shows the silicon solar device schematic with full-area rear carbonate electron heterocontacts. b) Presents the light J - V behavior measured under standard one sun conditions for cells without and with ≈ 1 nm carbonate interlayers. c) Shows the detailed electrical parameters (V_{oc} , J_{sc} , FF, and PCE) for different carbonate films.

in thermal stability among the six carbonates studied here. In contrast, only the solar cells with Cs₂C_xO_y and BaC_xO_y contacts survive the 1000 h damp heat test, maintaining >95% of their initial performance. This behavior might be related to the fact that the two metal ions have the largest atomic numbers of the six explored here.^[18]

In summary, six different alkali and alkaline earth metal carbonates have been demonstrated to function as effective and stable electron contacts for silicon solar cells, enabling significant gains in performance over a control device with Al directly on n-Si. It is further shown that all the carbonate/Al contacted solar cells are thermally stable up to 350 °C, and that two of the carbonate/Al contacts (Cs and Ba) pass the standard 1000 h damp heat test at 85 °C and 85% relative humidity. The high variety, low temperature deposition, and simple, yet effective, electron contact structure of these materials, pave the way for designing and fabricating novel cathodes for low-cost silicon solar cells.

Experimental Section

Carbonates films were thermally evaporated at a rate of 0.1 Å s⁻¹ and a base pressure of <1 × 10⁻⁶ Torr from a series of Sigma-Aldrich carbonate powder sources, as summarized below.

Material	Potassium carbonate	Rubidium carbonate	Caesium carbonate	Calcium carbonate	Strontium carbonate	Barium carbonate
Purity [%]	99.995	99.8	99.995	99.999	99.995	99.999

XPS characterization was performed on carbonate thin films on single-side polished c-Si wafers using a Kratos AXIS Ultra delay-line detector (DLD) system, under ultrahigh vacuum with a monochromatic Al K_α X-ray source and a hemispherical analyzer. Secondary electron cutoff measurements with X-ray excitation was employed for work function measurements. Voigt lineshapes were used to fit core level spectra, and film surface stoichiometry was extracted based on the resulting peak areas. A gold reference was used in the same session to verify instrument work function and to provide a reference for the work functions reported.

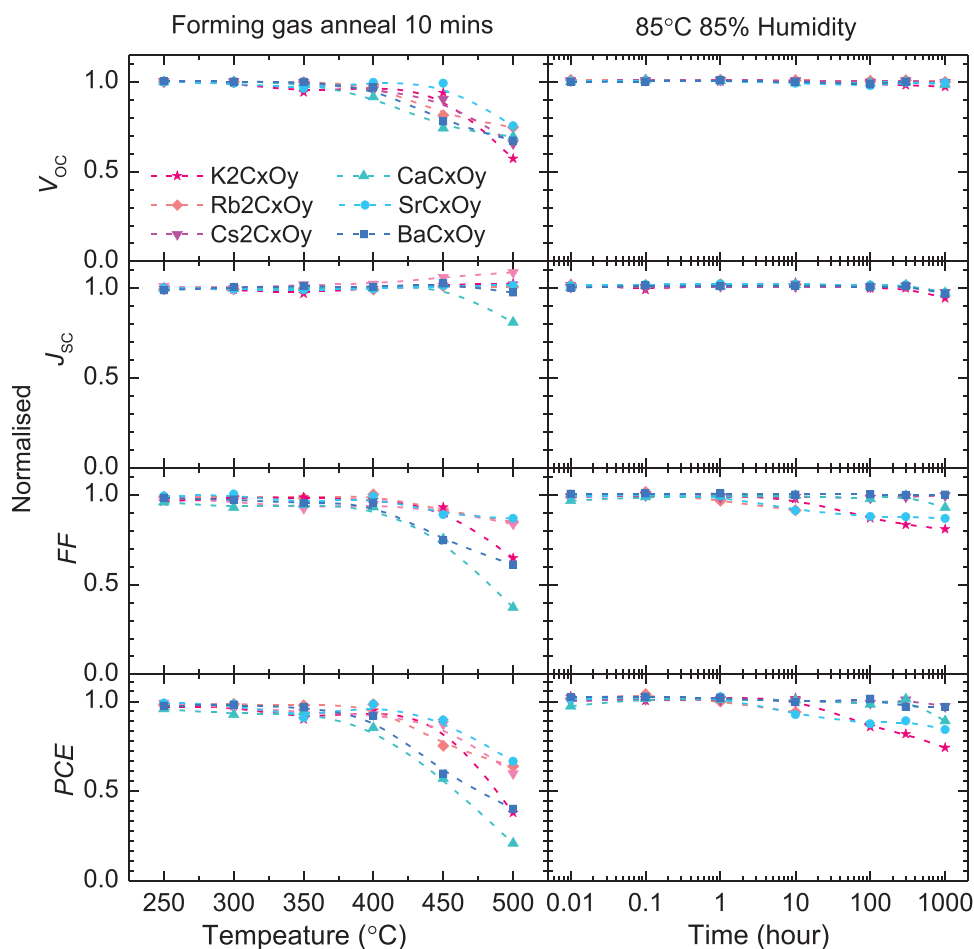


Figure 4. Thermal and humidity stability of the carbonate contacted photovoltaic cells. The relative changes in electrical parameters (V_{oc} , J_{sc} , FF, and PCE) are plotted as function of annealing temperature and damp heat test time.

Contact resistivity test samples for carbonates/Al electron contacts were fabricated on Czochralski (Cz) n-Si wafers. Shadow masks were used to pattern an array of circular pads with different diameters upon thermal evaporation. The rear of the contact samples was phosphorus diffused (n^+) to minimize the contribution of the rear Al/Si contact. A Keithley 2425 source-meter was used to conduct current-voltage (I - V) measurements at room temperature. The resistance versus diameter trend was fitted with a spreading resistance model, enabling extraction of contact resistance ρ_c .

Proof-of-concept solar cells were fabricated on Cz n-Si wafers with a resistivity of $\approx 1.0 \Omega\text{cm}$ and a thickness of $\approx 180 \mu\text{m}$. The sunward side of cells features an array of random pyramids,^[19–23] $\approx 110 \Omega \square^{-1}$ boron diffusion, and then $\approx 20 \text{ nm}$ atomic layer deposition (ALD) Al_2O_3 and $\approx 65 \text{ nm}$ plasma enhanced chemical vapour deposition (PECVD) silicon nitride.^[24] The rear silicon surfaces were then coated with the carbonates electron contacts (i.e., $\approx 1 \text{ nm}$ carbonates/200 nm Al). The front metal grid contacts with $10 \mu\text{m}$ width lines and 1.3 mm pitch were patterned via photolithography, followed by thermal evaporation of a Cr ($\approx 10 \text{ nm}$)/Pd ($\approx 10 \text{ nm}$)/Ag ($\approx 100 \text{ nm}$) stack, and finally thickened by Ag electroplating. The light J - V behavior was measured by a solar simulator from Sinton Instruments under standard one sun conditions (100 mW cm^{-2} , AM1.5 spectrum, 25°C), calibrated with a certified Fraunhofer CalLab reference cell.

Acknowledgements

This work was supported by the Australian Government through the Australian Research Council (Discovery Project: DP150104331) and

the Australia-US Institute for Advanced Photovoltaics (AUSIAPV) program under Grant No. ACAP6.9. Y.W. is holding Individual Fellowship from Australian Center of Advanced Photovoltaics (ACAP). The XPS characterization was performed at the Joint Center for Artificial Photosynthesis, supported through the Office of Science of the US Department of Energy under Award No. DE-SC0004993. Work at the Molecular Foundry was supported by the Office of Science, Office of Basic Energy Sciences, of the U.S. Department of Energy (Contract No. DE-AC02-05CH11231). A.J., M.H., and J.B. acknowledge funding from the Bay Area Photovoltaics Consortium (BAPVC).

Conflict of Interest

The authors declare no conflict of interest.

Keywords

alkali carbonate, alkaline earth metal carbonates, electron heterocontacts, silicon photovoltaics

Received: March 6, 2018

Revised: April 8, 2018

Published online:

- [1] D. K. Schroder, *Semiconductor Material and Device Characterization*, 3rd ed., John Wiley and Sons Inc., Hoboken, NJ **2006**.
- [2] S. M. Sze, K. K. Ng, *Physics of Semiconductor Devices*, John Wiley and Sons, New Jersey, USA **2006**.
- [3] Y. Zhang, R. Liu, S.-T. Lee, B. Sun, *Appl. Phys. Lett.* **2014**, *104*, 083514.
- [4] J. Bullock, M. Hettick, J. Geissbühler, A. J. Ong, T. Allen, C. M. Sutter-Fella, T. Chen, H. Ota, E. W. Schaler, S. De Wolf, C. Ballif, A. Cuevas, A. Javey, *Nat. Energy* **2016**, *1*, 15031.
- [5] J. Bullock, P. Zheng, Q. Jeangros, M. Tosun, M. Hettick, C. M. Sutter-Fella, Y. Wan, T. Allen, D. Yan, D. Macdonald, *Adv. Energy Mater.* **2016**, *6*, 1600241.
- [6] Y. Wan, C. Samundsett, J. Bullock, T. Allen, M. Hettick, D. Yan, P. Zheng, X. Zhang, J. Cui, J. A. McKeon, *ACS Appl. Mater. Interfaces* **2016**, *8*, 14671.
- [7] Y. Wan, C. Samundsett, J. Bullock, M. Hettick, T. Allen, D. Yan, J. Peng, Y. Wu, J. Cui, A. Javey, A. Cuevas, *Adv. Energy Mater.* **2017**, *7*, 1601863.
- [8] S. Avasthi, W. E. McClain, G. Man, A. Kahn, J. Schwartz, J. C. Sturm, *Appl. Phys. Lett.* **2013**, *102*, 203901.
- [9] X. Yang, P. Zheng, Q. Bi, K. Weber, *Sol. Energy Mater. Sol. Cells* **2016**, *150*, 32.
- [10] Y. Wan, S. K. Karuturi, C. Samundsett, J. Bullock, M. Hettick, D. Yan, J. Peng, P. R. Narangari, S. Mokkaipati, H. H. Tan, C. Jagadish, A. Javey, A. Cuevas, *ACS Energy Lett.* **2018**, *3*, 125.
- [11] J. Bullock, Y. Wan, Z. Xu, S. Essig, M. Hettick, H. Wang, W. Ji, M. Boccard, A. Cuevas, C. Ballif, A. Javey, *ACS Energy Lett.* **2018**, *3*, 508.
- [12] Y. Zhang, W. Cui, Y. Zhu, F. Zu, L. Liao, S.-T. Lee, B. Sun, *Energy Environ. Sci.* **2015**, *8*, 297.
- [13] J. Bullock, Y. Wan, M. Hettick, J. Geissbühler, J. Alison, O. D. Kiriya, D. Yan, T. Allen, J. Peng, Z. Xinyu, C. M. Sutter-Fella, S. D. Wolf, C. Ballif, A. Cuevas, A. Javey, presented at *IEEE 43rd Photovoltaic Spec. Conf. (PVSC)*, Portland, Oregon, June **2016**.
- [14] F. A. Cotton, G. Wilkinson, *Advanced Inorganic Chemistry*, John Wiley and Sons, New Jersey, USA **1988**.
- [15] A. V. Shchukarev, D. V. Korolkov, *Cent. Eur. J. Chem.* **2004**, *2*, 347.
- [16] J. Huang, Z. Xu, Y. Yang, *Adv. Funct. Mater.* **2007**, *17*, 1966.
- [17] R. H. Cox, H. Strack, *Solid-State Electron.* **1967**, *10*, 1213.
- [18] K. C. Kwon, K. S. Choi, B. J. Kim, J.-L. Lee, S. Y. Kim, *J. Phys. Chem. C* **2012**, *116*, 26586.
- [19] M. G. Coleman, W. L. Bailey, C. B. Harris, I. A. Lesk, *U.S. Patent No. 4137123*, **1979**.
- [20] O. Tabata, R. Asahi, H. Funabashi, K. Shimaoka, S. Sugiyama, *Sens. Actuators, A* **1992**, *34*, 51.
- [21] L. M. Landsberger, S. Naseh, M. Kahrizi, M. Paranjape, *J. Microelectromech. Syst.* **1996**, *5*, 106.
- [22] J. S. You, D. Kim, J. Y. Huh, H. J. Park, J. J. Pak, C. S. Kang, *Sol. Energy Mater. Sol. Cells* **2001**, *66*, 37.
- [23] P. Papet, O. Nichiporuk, A. Kaminski, Y. Rozier, J. Kraiem, J. F. Lelievre, A. Chaumartin, A. Fave, M. Lemiti, *Sol. Energy Mater. Sol. Cells* **2006**, *90*, 2319.
- [24] Y. Wan, K. R. McIntosh, A. F. Thomson, A. Cuevas, *IEEE J. Photovoltaics* **2013**, *3*, 554.